The *Drosophila drop-dead* gene is required for eggshell integrity

Short title: *drop-dead* and the *Drosophila* eggshell

Tayler D. Sheahan[1,#a], Amanpreet Grewal[1], Laura E. Korthauer[1,#b], Edward M. Blumenthal[1*]

[1] Department of Biological Sciences, Marquette University, Milwaukee, Wisconsin, United States of America

[#a]Current Address: Pittsburgh Center for Pain Research and Department of Neurobiology, University of Pittsburgh, Pittsburgh, Pennsylvania, United States of America

[#b]Current Address: Department of Psychiatry and Human Behavior, Alpert Medical School of Brown University, Providence, Rhode Island, United States of America

*Corresponding author

E-mail: edward.blumenthal@marquette.edu (EMB)

Abstract

The eggshell of the fruit fly *Drosophila melanogaster* is a useful model for understanding the synthesis of a complex extracellular matrix. The eggshell is synthesized during mid-to-late oogenesis by the somatic follicle cells that surround the developing oocyte. We previously reported that female flies mutant for the gene *drop-dead* (*drd*) are sterile, but the underlying cause of the sterility remained unknown. In this study, we examined the role of *drd* in eggshell synthesis. We show that eggs laid by *drd* mutant females are fertilized but arrest early in embryogenesis, and that the innermost layer of the eggshell, the vitelline membrane, is abnormally permeable to dye in these eggs. In addition, the major vitelline membrane proteins fail to become crosslinked by nonreducible bonds, a process that normally occurs during egg activation following ovulation, as evidenced by their solubility and detection by Western blot in laid eggs. In contrast, the Cp36 protein, which is found in the outer chorion layers of the eggshell, becomes crosslinked normally. To link the *drd* expression pattern with these phenotypes, we show that *drd* is expressed in the ovarian follicle cells beginning in mid-oogenesis, and, importantly, that all *drd* mutant eggshell phenotypes could be recapitulated by selective knockdown of *drd* expression in the follicle cells. To determine whether *drd* expression was required for the crosslinking itself, we performed *in vitro* activation and crosslinking experiments. The vitelline membranes of control egg chambers could become crosslinked either by incubation in hyperosmotic medium, which activates the egg chambers, or by exogenous peroxidase and hydrogen peroxide. In contrast, neither treatment resulted in the crosslinking of the vitelline membrane in *drd* mutant egg chambers. These results indicate that *drd* expression in the follicle cells is necessary for vitelline

46 membrane proteins to serve as substrates for peroxidase-mediated cross-linking at

47 the end of oogenesis.

Introduction

Animal epithelial cells produce an extracellular matrix (ECM) that must perform many roles, including as a structural support, barrier, and source of signaling molecules [1–3]. The eggshell of the insect *Drosophila melanogaster* is a model ECM consisting of five layers of protein, lipid, and carbohydrate [4]. Among its functions, the *Drosophila* eggshell serves as physical protection and a selective permeability barrier, provides patterning signals for the oocyte and developing embryo, and binds pheromones that prevent cannibalism by conspecific larvae [5–7]. Eggshell components are primarily synthesized by the follicle cells, a layer of somatic epithelial cells that surround the germline nurse cells and oocyte; together these three cell types make up the basic unit of oogenesis, the egg chamber.

The innermost layer of the eggshell is the proteinaceous vitelline membrane (VM). It is composed of six related structural proteins encoded by the genes *Vm26Aa*, *Vm26Ab*, *Vm26Ac*, *Vm32E*, *Vm34Ca*, and *Vml*, as well as other less abundant proteins [4,8–12]. While most VM components are produced by the follicle cells, at least three proteins, encoded by *fs(1)Nasrat* (*fs(1)N*), *fs(1)polehole* (*fs(1)ph*) and *closca* (*clos*), are secreted by the oocyte and become incorporated into the developing VM [13–15]. VM components are synthesized during mid-oogenesis (stages 8-11 of the 14 stages of oogenesis), followed by chorion components in stages 11-12 [4,16,17].

Following their synthesis and secretion, the proteins of the VM become cross-linked, forming a stable and insoluble matrix. The VM proteins are cross-linked to each other by disulfide bonds during the early stages of eggshell formation [11,18]. Immediately following ovulation and egg activation, VM proteins become cross-linked by non-reducible bonds, at least some of which are dityrosine bonds [19]. The non-

reducible cross-linking of the VM occurs in a matter of minutes as the egg moves down the oviduct; soluble VM proteins are never detected in freshly laid eggs [20,21]. While the formation of dityrosine bonds is typically catalyzed by a peroxidase [22–25], the enzyme responsible for VM crosslinking has not been identified.

The structural integrity of the *Drosophila* VM can be disrupted by mutations in several genes. Mutation of many of the genes encoding VM structural proteins causes gross VM abnormalities and collapse of the eggs [26–28], as do mutations in the cadherin *Cad99C* [29,30], which is localized to microvilli on the apical surface of the follicle cells, and the eggshell components *yellow-g* and *yellow-g2* [8,31]. Other mutations, in the genes encoding the minor eggshell components Nudel, Palisade (Psd), Clos, Fs(1)ph, and Fs(1)N, result in a disruption in VM protein cross-linking without altering overall VM integrity to the extent of causing eggs to collapse [13,14,20,32,33], however all of these mutations result in female sterility.

In this paper, we studied the role of the *drop-dead* (*drd*) gene in oogenesis. *drd* encodes a putative integral membrane protein of unknown function with homology to prokaryotic acyltransferases [34]. Mutation of *drd* causes a wide range of phenotypes, including female sterility, early adult death and neurodegeneration, defective food movement through the gut, and absence of a peritrophic matrix from the midgut [35–39]. The basis for female sterility has not previously been reported. Here we demonstrate that *drd* expression in the follicle cells is required for non-reducible cross-linking of the VM.

Materials and methods

Drosophila stocks and maintenance

All fly stocks were maintained on standard cornmeal-yeast-agar food (http://flystocks.bio.indiana.edu/Fly_Work/media-recipes/molassesfood.htm) at 25°C on a 12h:12h light-dark cycle. For RNAi experiments, a *UAS-Dcr-2* transgene was included in the genetic background of the flies in order to boost RNAi efficiency; the *drd*^{GD15915} *UAS-Dcr-2* and *UAS-Dcr-2 drd*^{GD3367} lines were created previously by recombination between VDRC stocks *w*^{1118}*;P{GD3367}v37404* (FBst0461992) and *w*^{1118}*; P{GD15915}v51184* (FBst0469325) and Bloomington stock *w*^{1118}*; P{UAS-Dcr-2.D}2* (FBst0024650, RRID:BDSC_24650) [40,41]. The *w*; P{w*$^{+mW.hs}$*GAL4=GawB}CY2* stock (FBti0007266, referred to as *CY2-GAL4*) was provided by Dr. Celeste Berg. Other stocks (*w*^{1118}*; P{UAS-GFP.nls}14* (FBst0004775, RRID:BDSC_4775), *P{w*$^{+mW.hs}$*=GawB}T155* (FBst0005076, RRID:BDSC_5076, referred to as *T155-GAL4*), *w* ovo*^{D1} *v*^{24} *P{w*$^{+mW.hs}$*=FRT(w*^{hs}*)}101/C(1)DX, y*^{1} *f*^{1}*; P{ry*$^{+t7.2}$*=hsFLP}38* (FBst0001813, RRID:BDSC_1813), and *y*^{1} *w* v*^{24} *P{w*$^{+mW.hs}$*=FRT(w*^{hs}*)}101* (FBst0001844, RRID:BDSC_1844)), were obtained from the Bloomington *Drosophila* Stock Center. Creation of the *drd-GAL4* driver transgene has been reported previously [36]. The genes and alleles referenced in this work include *drd* (FBgn0260006), *drd*^{lwf} (FBal0193421), *drd*^{1} (FBal0003113). Stocks were not outcrossed prior to this study.

drd^{1} sequencing

Whole-fly RNA was prepared from Canton S and *drd*^{1} homozygous adults using Trizol reagent (ThermoFisher Scientific, Waltham, MA). RNA was treated with

DNase (ThermoFisher Scientific, Waltham, MA) and cDNA was synthesized (qScript cDNA supermix, Quantabio, Beverly, MA). Primers for amplification of the exon 8/9 junction were: CG5652 6a 5' GAT CGC CTG GTG TTT GTT TT 3' and CG5652 6b 5' TTC GCT GGG GAT CAC TAA AC 3'.

Egg-laying assay

Groups of 1-3 homozygous drd^{1}/drd^{1} or drd^{lwf}/drd^{lwf} females were mated with Canton S males and placed on either regular food or food supplemented with yeast paste. Flies were transferred to new vials daily until they died, and the number of eggs laid was recorded. Because groups of three flies were assayed together in early experiments, we analyzed the data twice—once assuming that all eggs were laid by a single fly (model 1) and once assuming that egg-laying was distributed evenly among all flies in a vial (model 2). The conclusions about the proportion of flies that laid eggs were the same in both analyses.

Analysis of embryogenesis

Females were mated with sibling males, and eggs were collected overnight (16.5-18.5 hr) on apple juice agar plates supplemented with yeast paste [42]. Flies were removed and the eggs were allowed to develop for an additional 2-6 hr. Eggs were then covered in halocarbon 700 oil (Sigma-Aldrich, St. Louis, MO) and scored for collapsed vs turgid. Turgid eggs were scored for fertilized vs unfertilized, and fertilized eggs were scored for pregastrulation vs postgastrulation [42].

Generation of *drd* germline clones

Germline mitotic clones mutant for *drd* were generated using the FLP/FRT-dominant female sterile technique as described [43]. The drd^{lwf} allele was first recombined onto the same chromosome as an FRT site by crossing *w* drd^{lwf} x *y w v P{FRT}101*. Following the establishment of a stock carrying this recombinant chromosome, *w* drd^{lwf} *P{FRT}101/FM7a* females were crossed with *w* ovo^{D1} *v P{FRT}101; hs-FLP* males. The resulting *w* drd^{lwf} *P{FRT}101/w* ovo^{D1} *v P{FRT}101; hs-FLP/+* embryos were heat shocked for 2 hr at 37°C to induce FLPase expression and mitotic recombination, raised to adulthood, and crossed with Canton S males to assay for fertility. Control embryos of the same genotype were not heat-shocked. Male progeny of the germline clones were collected and their lifespan measured to confirm the presence of the drd^{lwf} mutation.

Visualization of *drd* expression pattern

yw drd-GAL4/FM7i-GFP females were crossed with *w; UAS-GFP.nls* males. Female progeny were crossed with sibling males. Ovaries from females 3-6 days post-eclosion were dissected in insect Ringers and separated into individual egg chambers. Samples were imaged on a Nikon A1 Confocal Microscope (Nikon, Tokyo, Japan) with NIS-Elements AR software (Nikon).

Neutral red permeability assay

Eggs were collected on apple-juice agar plates for 2-19 hr, placed into a stainless steel mesh basket, and rinsed with PBS. Eggs were dechorionated by gently shaking in a 50% bleach solution for 3 min followed by rinsing with PBS; exposure to bleach was only 1 min for drd^{1}/drd^{1} and $drd^{1}/FM7c$. The dechorionated eggs were counted, stained with 5 mg/mL neutral red (VWR, Radnor, PA) in PBS for

10 min, rinsed with PBS, and scored as stained or unstained. No correlation was observed between the duration of the egg collection and the staining results. See S1 Text for detailed protocol.

Western blot analysis

Egg chambers were dissected in PBS or eggs were collected on apple-juice agar plates, and samples were homogenized in 80µL of 20mM Tris-HCl (pH7.5), 0.15 M NaCl, 100 mM DTT. Samples were then heated at 100°C for 5 min, centrifuged (14,000g, 1 min), and the resulting pellet discarded. One quarter volume 5x SDS-PAGE loading buffer was added to each sample, and they were again heated for 5 min at 100°C and stored at -20°C until further use. Prior to electrophoresis, samples were treated with 5% β-mercaptoethanol and heated for 3 min at 100°C. For any gel, the same amount of egg chamber equivalents of each sample was loaded, typically ranging from 1-5 egg chamber equivalents. Following separation via SDS-PAGE (12%, Mini PROTEAN 3 System, Bio-Rad, Hercules, CA), proteins were transferred to PVDF membrane for 1hr using a Genie electroblot chamber (Idea Scientific, Minneapolis, MN). Membranes were then washed for 10 min in PBS and blocked overnight in PBS/0.05% Tween-20 (PBS-T)/ 5% nonfat dry milk at 4°C. After blocking, two 5 min washes in PBS-T were conducted prior to 1 hr incubation in primary antibody diluted in PBS-T/1% BSA. Membranes were then washed in PBS-T, once for 15 min, and four times for 5 min, followed by a 1 hr incubation in secondary antibody (ECL HRP-linked donkey anti-rabbit IgG, 1:10,000, Cytiva Life Sciences, Marlborough, MA). Again one 15 min and four 4 min washes in PBS-T were conducted and antibody signals were detected via chemiluminescence (ECL Prime Western Blotting System, Cytiva Life Sciences, Marlborough, MA).

Primary polyclonal rabbit antibodies were provided by Dr. Gail Waring and were previously characterized antibodies against Cp36 and Vm26Ab [9].

Immunostaining

drd^{1} heterozygous and homozygous females were collected on the day of eclosion on placed on yeast paste with sibling males for two days. Ovaries were immunostained as described [15], except that fixation was performed with 4% paraformaldehyde in PBS rather than formaldehyde in PBS/Triton X-100. Anti-Vm26Ab antibody was used at 1:5000, and the secondary antibody was Alexafluor 488 goat anti-rabbit IgG (1:400) (Invitrogen, Carlsbad, CA). Samples were imaged on a Nikon A1 Confocal Microscope (Nikon, Tokyo, Japan) with NIS-Elements AR software (Nikon). Images were analyzed in ImageJ v2.9.0, and the analyzer was blind to genotype. VM staining intensity was determined in stage 9 and 10A egg chambers by measuring mean pixel brightness in a 1mm x 5 mm rectangle of the anterior lateral oocyte margin. Within each genotype, there was no significant correlation between either VM width or staining intensity and developmental stage (as measured by the oocyte length/width ratio), allowing us to pool data across developmental stages for comparison between genotypes.

In vitro egg activation

To stimulate egg production, *drd*^{1}*/FM7c* and *drd*^{1}*/drd*^{1} females were placed on yeast paste and mated with sibling males 3-5 days before dissection. Egg activation *in vitro* was performed using the method of Page and Orr-Weaver [44]. Stage 14 egg chambers were dissected in isolation buffer (55 mM NaOAc, 40 mM KOAc, 110 mM sucrose, 1.2 mM $MgCl_2$, 1 mM $CaCl_2$, 100 mM Hepes, pH 7.4 (NaOH)). Egg

chambers were then incubated for 10 min in hypo-osmotic activating buffer (3.3 mM NaH_2PO_4, 16.6 mM KH_2PO_4, 10 mM NaCl, 50 mM KCl, 5% PEG 8000, 2 mM $CaCl_2$, pH 6.4 (1:5 NaOH: KOH)) and then transferred into modified Zalokar's buffer for 30 min (9 mM $MgCl_2$, 10 mM $MgSO_4$, 2.9 mM NaH_2PO_4 0.22 mM NaOAc, 5 mM glucose, 27 mM glutamic acid, 33 mM glycine, 2 mM malic acid, 7 mM $CaCl_2$, pH 6.8 (1:1 NaOH: KOH)). To test for eggshell crosslinking, egg chambers were then incubated in 50% bleach for 5 min and scored as intact, leaky, or completely dissolved. In some experiments, hydrogen peroxide (0.006-0.06%) was included in both the activating and Zalokar's buffer.

In a second series of experiments, the activating buffer incubation was omitted. Egg chambers were dissected and manually dechorionated in isolation buffer and then incubated for 30 min in Zalokar's buffer containing 4.5% hydrogen peroxide and 1 mg/ml horseradish peroxidase (VWR, Radnor, PA) before bleaching as above.

Data analysis and statistics

Data were graphed and analyzed using GraphPad Prism v9 for Windows (GraphPad Software, San Diego, CA, www.graphpad.com). A p value of <0.05 was used as the threshold for statistical significance.

Results

Identification of the *drd*^{1} mutation

The experiments in this study utilize flies carrying the two most severe alleles of *drd*: *drd*^{lwf} and *drd*^{1}. The mutation in the latter of these alleles not been molecularly characterized, although we previously reported that there were no alterations in the protein coding sequence [34]. Further sequencing of the final 5 introns and the ends of the first three large introns revealed six differences between *drd*^{1} and wild-type. One of these, a T to A transversion in the final intron, is predicted to create a strong ectopic splice acceptor site and result in the inclusion of an additional 10 nucleotides in the spliced transcript (S1 Fig) (www.fruitfly.org/seq_tools/splice.html) [45]. This aberrant splicing of the *drd* transcript in *drd*^{1} mutants was confirmed by RT-PCR. Virtual translation of the mutant transcript predicted that the final 76 amino acids of the Drd protein are replaced with a novel sequence of 45 amino acids in the *drd*^{1} mutant.

Sterility of *drd* mutant females

We have previously reported that females homozygous for severe *drd* alleles are sterile and rarely lay eggs, and their ovaries contain very few vitellogenic egg chambers [34]. We hypothesized that these phenotypes could be an effect of the starvation observed in *drd* mutant flies, as opposed to a direct phenotype of *drd* mutation. Consistent with this hypothesis, feeding females a high protein diet (yeast paste) stimulated egg-laying in a subset of flies. Yeast paste increased the percentage of *drd*^{lwf} females, but not *drd*^{1} females, that laid eggs, and it increased by

more than 30-fold the median number of eggs laid during their lifetime by those *drd*^{1} and *drd*^{lwf} homozygous females that laid eggs (S2 Fig).

Despite the improvement in egg-laying, *drd* homozygous females fed with yeast paste remained sterile. Eggs were collected overnight from mated *drd*^{1} heterozygotes and homozygotes and allowed to develop for an additional two hr before examination for progression through embryogenesis. As shown in Table 1, a significantly higher number of eggs laid by homozygotes were collapsed ($p<0.0001$, Fisher's exact test). Of the turgid eggs, the large majority were fertilized, and the rate of fertilization was not affected by the mother's genotype ($p=0.30$, Fisher's exact test). However, virtually no fertilized eggs laid by homozygotes underwent gastrulation, in contrast to embryos laid by heterozygotes ($p<0.0001$, Fisher's exact test). Thus, the sterility of *drd* mutant females appears to result from early embryonic arrest.

Table 1. Sterility of *drd* mutant females

Maternal genotype (# of eggs)	*drd*^{1}/*FM7c* (164)	*drd*^{1}/ *drd*^{1} (293)
Collapsed (% of total)	0.6%	17.7%
Unfertilized (% of turgid eggs)	7.5%	11.2%
Pre-gastrulation (% of fertilized eggs)	6.8%	99.0%
Post-gastrulation (% of fertilized eggs)	93.2%	1.0%

Table 1: Embryonic arrest in eggs laid by *drd*^{1} females. The second row indicates the percent of all eggs that were collapsed or flaccid. The following row indicates the percent of turgid eggs that were unfertilized (4 eggs from heterozygotes and 9 from homozygotes could not be scored and were excluded). The final two rows indicate

279 the percent of fertilized eggs that were scored as pre-gastrulation and post-
280 gastrulation, respectively.
281

282 Expression of *drd* in the egg chamber

283 To determine whether *drd* expression was required in the germline or soma
284 for female fertility, we created germline clones of drd^{lwf}. Almost all of these females
285 (15/17) were fertile when crossed with wild-type males, while non-heat shocked
286 controls were all sterile (n=28), indicating that *drd* expression is not required in the
287 female germline for fertility. The male progeny of these clones were short-lived
288 (median lifespan of 4 days, n=55), as would be expected for males hemizygous for
289 drd^{lwf}, confirming that the germline of these clones was mutant for *drd*.
290 Consistent with the germline clone analysis, driving a GFP reporter with a *drd-*
291 *GAL4* transgene resulted in labeling of all ovarian follicle cells (Fig 1). Visible
292 reporter expression appeared at stage 10B and persisted for the remainder of
293 oogenesis.
294

295 **Fig 1. Expression of *drd* in ovarian follicle cells.** The image shows a maximum
296 intensity projection of one stage 14 (top) and two stage 10B egg chambers in which
297 expression of a nuclear GFP reporter is driven by *drd-GAL4*. No staining was seen in
298 the nurse cell nuclei located in the anterior half of each stage 10B egg chamber (*).
299 No staining was seen in egg chambers from sibling control females lacking the *drd-*
300 *GAL4* driver (S3 Fig).
301

302 Abnormal eggshell development in *drd* mutant females

Because a significant number of eggs laid by *drd* mutants were collapsed and because *drd* expression was observed in the follicle cells and not the germline, we next examined the integrity of the eggshell, a structure synthesized by the somatic follicle cells. The integrity of the inner layer of the eggshell, the VM, was assayed by staining dechorionated eggs with neutral red, a dye that is normally excluded by the VM [20]. Virtually no eggs laid by drd^{1} and drd^{lwf} heterozygotes lysed during dechorionation (1-3%) or were stained with neutral red (3-4%) (Fig 2). In contrast, eggs laid by homozygotes of either *drd* allele showed a high susceptibility to lysis during dechorionation (31-42%), and the large majority of surviving eggs were permeable to neutral red (71-90%). A small fraction of eggs (4-11%) were not dechorionated upon treatment with bleach and could not be assessed for dye exclusion, but the abundance of such eggs was not affected by the genotype of the mother (p=0.19, Chi-square test).

Fig 2. Neutral red staining of eggs laid by *drd* homozygous and heterozygous females. (A) fraction of eggs that lysed during bleach treatment. (B) fraction of eggs that were stained with neutral red after successful dechorionation. ****: significant difference between eggs laid by heterozygotes vs homozygotes, p<0.0001, Fisher's exact test. 135-249 eggs per genotype.

As a direct test of the incorporation of eggshell proteins into an insoluble cross-linked matrix, we performed Western blots on lysates of staged egg chambers and laid eggs. An antibody against the chorion protein Cp36 detected the expected pattern of staining in samples from $drd^{1}/FM7c$ heterozygous females (Fig 3) [9]. Soluble Cp36 protein was not detected at stage 10 of oogenesis, which is before

chorion proteins such as Cp36 begin to be expressed, but Cp36 was detected in stage 14 lysates, when the protein is present in the chorion but has not yet been fully cross-linked. In lysates from eggs collected either 3 or 6 hr after deposition, Cp36 was not detectable, consistent with complete cross-linking of the protein into the insoluble chorion. The same pattern of staining was observed in lysates from eggs and egg chambers from *drd*^{1} homozygotes (Fig 3), indicating that crosslinking of the chorion, or at least of the specific protein Cp36, is not affected by mutation of *drd*.

Fig 3. Western blot of the chorion protein Cp36 in *drd* mutant and control egg chambers and eggs. Stage 10 and 14 egg chambers were dissected from *drd*^{1}/*drd*^{1} mutant and *drd*^{1}/*FM7c* heterozygous females, and eggs laid by these females were collected 0-3 and 0-6 hr after oviposition (lanes 3 and 7 and lanes 4 and 8). 4 eggs or egg chambers per lane, 1:5000 primary antibody dilution.

In contrast to the chorion, crosslinking of VM proteins was clearly abnormal in eggs laid by *drd* mutant homozygotes. Fig 4A shows the pattern of staining observed in egg chambers and eggs from heterozygous controls, using an antibody raised against the VM protein Vm26Ab [9]. This antibody has been reported to cross-react with multiple VM proteins due to their high degree of sequence similarity [18,46], and we typically observed multiple bands on Western blots. As expected, staining was observed in lysates from stage 10 egg chambers, when the VM proteins are not yet crosslinked, and from stage 14, when the VM proteins are crosslinked by disulfide bonds but are soluble in the presence of reducing agents. In laid eggs from heterozygotes, no soluble VM proteins were observed, consistent with the formation of nonreducible dityrosine bonds among VM proteins during ovulation and egg

activation. In lysates of laid eggs from *drd*^{1} homozygotes, VM proteins were detected on the Western blot, indicating that these proteins are not fully crosslinked in the absence of *drd* expression. We observed solubility of VM proteins in laid eggs of *drd*^{1} homozygotes in seven Western blots representing five biological replicates. The decrease in signal seen in Fig 4A with increasing time after oviposition (compare lanes 3 and 4) was not consistently observed.

Fig 4. Western blots against vitelline membrane proteins in *drd* mutant and control egg chambers and eggs. (A) Western blot of samples treated with reducing agents with an antibody raised against Vm26Ab. Samples include stage 10 and 14 egg chambers dissected from *drd*^{1}/*drd*^{1} mutant and *drd*^{1}/*FM7c* heterozygous females, and eggs laid by these females were collected 0-3 and 0-6 hr after oviposition. 4 eggs or egg chambers per lane, 1:10,000 primary antibody dilution. (B) Western blot from egg chambers solubilized in the absence of reducing agent and probed with an antibody against Vm26Ab. Samples include stage 10 and 14 egg chambers dissected from *drd*^{1}/*drd*^{1} mutant and *drd*^{1}/*FM7c* heterozygous females. 2 egg chambers per lane, 1:10,000 primary antibody dilution.

To assay for the formation of disulfide bonds among VM proteins during oogenesis, lysates were prepared from stage 10 and 14 egg chambers in the absence of reducing agents. Mutation of *drd* did not alter the pattern of immunostaining observed under these conditions (Fig 4B). Soluble protein was detected at stage 10 but not at stage 14, indicating that VM proteins are cross-linked by reducible bonds during oogenesis in both *drd* homozygotes and heterozygotes.

We performed immunostaining of stage 9 and 10A egg chambers against Vm26Ab to determine whether the appearance of the developing VM is altered in *drd* mutants (Fig 5A, B). We observed no significant effect of genotype on either the staining intensity (p=0.14, Mann-Whitney test) or width (p=0.33, t-test) of the VM (n=20-22 samples per genotype). There were also no obvious morphological differences in the egg chambers between the two genotypes. However, drd^1 homozygous egg chambers were slightly but significantly smaller than heterozygous controls. We used the size ratio of anterior-posterior length/lateral width of each oocyte as a measure of progression through oogenesis, as this ratio increases during stages 9 and 10A (Fig 5C). Anterior-posterior length was significantly linearly correlated with the size ratio for each genotype (p<0.0001, F test). The slope of the relationship did not differ between the two genotypes (p=0.88) but the intercept did differ (p=0.02), corresponding to a decrease in size of homozygous oocytes of approximately 15%.

Fig 5. Immunostaining of the VM. Stage 10A egg chambers from a drd^1 heterozygote (A) and homozygote (B) were stained with the anti-Vm26Ab antibody. The rectangle indicates the region in which staining intensity and eggshell width were measured. Oo: oocyte; nc: nurse cells; fc: follicle cells. (C) Plot of the size ratio of anterior-posterior length/lateral width for each oocyte as a function of the anterior-posterior length, showing the slight difference between drd^1 heterozygotes and homozygotes.

Follicle cell knockdown of *drd* recapitulates mutant phenotypes

Our finding that *drd* expression is required in the soma for female fertility, coupled with the known role of the somatic follicle cells in the synthesis of the eggshell, suggested that all of the *drd* mutant phenotypes related to fertility and eggshell assembly could be associated with the expression of *drd* in the follicle cells. To test this, we knocked down *drd* expression in the follicle cells, using two pan-follicle cell GAL4 drivers, *CY2-GAL4* and *T155-GAL4*, and two inducible *drd* RNAi transgenes, drd^{GD3367} and $drd^{GD15915}$, that we have previously shown to be effective at knocking down *drd* expression [40]. Females heterozygous for a GAL4 driver and an RNAi transgene (referred to as knockdown females) and sibling control females that lacked the RNAi transgene were mated with sibling males, and their eggs were scored for fertilization, embryonic development, eggshell integrity, and crosslinking.

As shown in Table 2, a greater percentage of eggs from knockdown females were collapsed compared with sibling controls, and virtually all fertilized eggs from knockdown females were arrested pre-gastrulation, as was seen in mutant females (Fisher's exact test, $p<0.0001$ for each genotype). The proportion of eggs laid by knockdown females that was fertilized was not significantly different than that of sibling controls for three of the four genotypes tested, with a small but significant effect on fertilization for one combination of GAL4 driver and RNAi transgene. Despite the near-universal arrest of eggs from knockdown females early in oogenesis in this assay, we did occasionally observe larvae in vials of knockdown females carrying *T155-GAL4* and either of the RNAi-transgenes, indicating that these females were not fully sterile. Knockdown females carrying the *CY-GAL4* driver, like *drd* mutant females, appeared to be completely sterile.

Table 2. Sterility of *drd* knockdown females

427

Maternal genotype (# of eggs)	*w; UAS-Dcr-2 drd^{GD3367}/+; T155-GAL4/+* (188)	*w; drd^{GD15915} UAS-Dcr-2/+; T155-GAL4/+* (155)	*w; UAS-Dcr-2 drd^{GD3367}/CY2-GAL4* (169)	*w; drd^{GD15915} UAS-Dcr-2/CY2-GAL4* (206)
Collapsed (% of total)	32.4%****	43.9%****	21.9%****	24.3%****
Unfertilized (% of turgid eggs)	6.1%	10.0%	7.8%*	4.8%
Pre-gastrulation (% of fertilized eggs)	100%****	98.6%****	100%****	96.4%****
	w; CyO/+; T155-GAL4/+ (153)	*w; CyO/+; T155-GAL4/+* (221)	*w; CY2-GAL4/CyO* (238)	*w; CY2-GAL4/CyO* (163)
Collapsed (% of total)	0%	0.5%	0.4%	0.6%
Unfertilized (% of turgid eggs)	3.4%	10.3%	2.2%	4.5%
Pre-gastrulation (% of fertilized eggs)	0.7%	1.0%	1.3%	2.7%

428 Table 2: Embryonic arrest upon knockdown of *drd* expression in the follicle cells.
429 Knockdown females (top four rows) and sibling controls (bottom four rows) were
430 mated with sibling males, and eggs were collected and scored as in Table 1. The
431 number of uncollapsed but unscorable eggs that were excluded from further analysis
432 varied from 4-13 among each of the eight genotypes. ****: different from sibling
433 controls, $p<0.0001$, Fisher's exact test, *: $p=0.024$.

Tests of eggshell integrity by neutral red exclusion demonstrated that eggs laid by follicle cell knockdown females showed a similar defect to those laid by *drd* mutants. As shown in Fig 6, we observed a significant and consistent increase in the proportion of eggs that were permeable to neutral red compared to those laid by sibling controls (Fig 6C). The percent of eggs that lysed upon dechorionation was also significantly different between knockdown and sibling control females for three of the four genotypes (Fig 6A). Finally, and in contrast to the data from *drd* mutants, we observed a small but significant increase in the fraction of eggs from knockdown females that were successfully dechorionated relative to sibling controls in two of the four genotypes (Fig 6B).

Fig 6. Neutral red staining of eggs following *drd* knockdown. Data from eggs laid by *drd* knockdown (striped orange and green bars) and sibling control (solid black bars) females. (A) fraction of eggs that lysed during bleach treatment. (B) fraction of eggs that were successfully dechorionated. (C) fraction of eggs that were stained with neutral red after dechorionation. Significant difference between eggs laid by knockdown females and sibling controls by Fisher's exact test are indicated: **** $p<0.0001$, *** $p=0.0006$, ** $p=0.0016$, * $p=0.015$. 195-225 eggs per genotype.

Crosslinking of VM proteins in laid eggs and stage 14 egg chambers from knockdown and control females was assayed by Western blot with the antibody against Vm26Ab as described above. A representative blot is shown in Fig 7. Knockdown females carrying the *CY2-GAL4* driver showed a phenotype identical to that of *drd* mutants: we consistently observed soluble VM proteins in both stage 14

egg chambers and laid eggs, while soluble VM proteins were only observed in the stage 14 chambers of sibling controls (3 biological replicates with *drd*^{GD3367} and 2 with *drd*^{GD15915}). In contrast, soluble VM proteins were detected in only some samples of eggs laid by knockdown females carrying the *T155-GAL4* driver (2/4 biological replicates with *drd*^{GD3367} and 1/3 with *drd*^{GD15915}).

Fig 7. Western blots against vitelline membrane proteins in *drd* knockdown egg chambers and eggs. Blots were probed with an antibody raised against Vm26Ab. Samples include stage 14 egg chambers dissected from, and eggs laid by, females in which the inducible *drd* RNAi transgene, *drd*^{GD3367}, was driven by either the *CY2-GAL4* or *T155-GAL4* driver, or sibling controls lacking the RNAi transgene. Lanes are marked “st 14” for egg chambers and “e” for eggs. 2 eggs or egg chambers per lane, 1:25,000 primary antibody dilution. Eggs were collected between 0-4.5 hr after oviposition.

Cross-linking of VM in isolated egg chambers

To determine whether the *drd* cross-linking defect persists in isolated egg chambers, we dissected stage 14 egg chambers and activated them *in vitro* by exposure to hypo-osmotic medium as previously reported [44]. VM cross-linking was assayed by then incubating the egg chambers in 50% bleach (Fig 8A). All egg chambers dissected from *drd*^{1}*/FM7c* control females were successfully cross-linked following hypo-osmotic treatment. In contrast, all egg chambers dissected from *drd*^{1} homozygotes completely dissolved in bleach. Additional egg chambers were dissected from homozygotes and treated with 0.006-0.06% hydrogen peroxide during treatment with hypo-osmotic medium and for 30 min afterwards, and all these

egg chambers also dissolved completely in bleach. It is noteworthy that the *drd* mutant phenotype is more severe in egg chambers activated *in vitro* than *in vivo*, as most eggs laid by *drd* homozygous females remain intact upon treatment with bleach (see Fig 2 above).

Fig 8. Results of *in vitro* egg activation. The figure indicates the number of egg chambers dissected from each female genotype that remained intact, became leaky, or dissolved in 50% bleach after treatment with hypo-osmotic medium (A) or hydrogen peroxide and horseradish peroxidase (B).

We then attempted to directly cross-link the VM of stage 14 egg chambers by treatment with hydrogen peroxide and peroxidase. Stage 14 egg chambers were dissected, manually dechorionated, and treated with peroxide/peroxidase without exposure to hypo-osmotic medium (Fig 8B). Egg chambers dissected from *drd*^{1}*/FM7c* control females and treated with 1 mg/ml peroxidase and 4.5% hydrogen peroxide all survived a subsequent challenge with bleach. This cross-linking was not due to inadvertent activation of the egg chambers during dechorionation, as omitting the hydrogen peroxide from the incubation resulted in all egg chambers dissolving in bleach. Egg chambers from *drd*^{1} homozygotes treated with peroxide/peroxidase as above all dissolved in bleach.

Discussion

We have demonstrated that expression of *drd* in the ovarian follicle cells is both necessary and sufficient for female fertility and the progression of embryonic development beyond gastrulation. Germline clones in which *drd* expression is restricted to somatic cells are fertile, while knockdown of *drd* expression specifically in the follicle cells recapitulates the mutant phenotype. These results are consistent with those of Kim et al, who reported expression of *drd* in the follicle cells [47]. Furthermore, we have shown that *drd* expression in the follicle cells is required for proper development of the VM layer of the eggshell. In the absence of such expression, many eggs collapse, and the remaining eggs have a fragile VM that fails to act as a permeability barrier. Several major VM proteins—specifically those recognized by the antibody used in these studies—remain soluble in the presence of reducing agents, indicating that they have not been incorporated into the insoluble network of cross-linked proteins seen in the wild-type VM. The variable solubility phenotype observed with knockdown of *drd* with the *T155-GAL4* driver is consistent with the fertility of some of these knockdown females and suggests that *T155-GAL4* is not as effective as the *CY2-GAL4* driver in knocking down *drd* expression. The difference in strength of these two driver lines has been reported previously [48].

The solubility of VM proteins in eggs laid by *drd* mutants indicates a defect in the peroxidase-mediated cross-linking that normally occurs upon egg activation while the egg is transiting down the oviduct. We have no evidence that egg activation itself is defective, as the eggs were able to complete the early stages of embryogenesis. Our data don't address the connection between defective VM cross-linking and embryonic arrest, and it remains possible that embryonic arrest is an independent *drd* phenotype. However, this same pairing of phenotypes has been reported with

another eggshell mutant. Females mutant for *psd*, which encodes a minor VM protein, also lay eggs with a VM cross-linking defect and that arrest pre-gastrulation and show a chromatin margination phenotype similar to that induced by anoxia [32]. Thus, it is possible that defective VM cross-linking is a direct cause of early developmental arrest.

A published microarray study of ovarian gene expression has reported that *drd* expression in the egg chamber begins at stage 8 of oogenesis, peaks at stages 10A and 10B, and then declines [16]. The timing of *drd* expression therefore parallels the synthesis and secretion of VM proteins by the follicle cells. The pattern of reporter expression shown in Fig 1 is consistent with the microarray data. We observed GFP fluorescence starting at stage 10B and persisting through the rest of oogenesis; one would expect both a delay between the onset of GFP expression and significant accumulation in the follicle cell nuclei and persistence of the protein after gene expression is downregulated. The Drd protein is unlikely to be a component of the VM, as it is predicted to be an integral membrane protein and is reported to be localized to an intracellular compartment [34,47]. Drd is also unlikely to be directly involved in the cross-linking process, which occurs at the end of oogenesis when *drd* expression is very low. Rather, our data suggest that the failure of VM proteins to become cross-linked in *drd* mutants could be due to an absence of some modification of the VM proteins in the follicle cells prior to secretion. The results of our final experiment are consistent with this hypothesis. Incubation of stage 14 egg chambers with peroxide and peroxidase resulted in cross-linking of the VM in egg chambers from wild-type but not mutant females. Thus, VM proteins synthesized and secreted from *drd* mutant follicle cells appear to be poor substrates for peroxidase-mediated cross-linking for reasons still to be determined.

One interesting finding from our final experiment is that egg chambers from *drd* mutant females dissolve immediately in bleach after activation *in vitro* with hypoosmotic medium. In contrast, eggs laid by *drd* mutant females mainly survive bleaching, even though their VMs are permeable to neutral red. The contrast between these two results indicates that hypoosmotic treatment *in vitro* does not fully recapitulate the activation process *in vivo* even though the two processes appear to give identical results in wild-type flies [44]. The *drd* mutant female could prove to be a useful system for identifying additional factors that influence eggshell maturation during ovulation and oviposition.

In addition to characterizing the effect of *drd* mutations on oogenesis, we have identified the molecular defect in the severe drd^{1} allele as a point mutation in the final intron that disrupts the normal splicing of exons 8 and 9. The aberrant splicing replaces the final 76 residues of the 827 amino acid Drd protein with a novel sequence. Because drd^{1} is phenotypically identical to drd^{lwf}, a nonsense mutation that eliminates all but the first 180 amino acids, our finding highlights the importance of the C-terminal of Drd in protein function, stability, or localization. In contrast, the drd^{W3} and $In(1)drd^{x1}$ alleles, which eliminate the first exon and at least the first 125 amino acids, are phenotypically less severe [34].

The biochemical function of the Drd protein remains unknown. However, this study highlights two themes that are emerging from our studies of this gene. First, *drd* expression appears to be required in a number of different epithelial tissues, including the ovarian follicle cells for oogenesis, the anterior midgut for digestive function, and the respiratory tracheae for brain integrity. Second, *drd* expression is required for the formation of extracellular barrier structures, as *drd* mutants show defects both in the eggshell and in the peritrophic matrix of the midgut. Given the

579 amount of information known about eggshell formation, the ovary is an excellent

580 system for further studies of *drd* function.

Acknowledgments

We thank Dr. Celeste Berg for the CY2-GAL4 stock, Drs. Gail Waring and Anita Manogaran for antibodies and helpful discussions, and Anika Benske for technical assistance. Stocks obtained from the Bloomington Drosophila Stock Center (NIH P40OD018537) and the Vienna Drosophila Resource Center were used in this study.

References Cited

1. Yue B. Biology of the extracellular matrix. J Glaucoma. 2014;23: S20–S23. doi:10.1097/ijg.0000000000000108

2. Broadie K, Baumgartner S, Prokop A. Extracellular matrix and its receptors in Drosophila neural development. Dev Neurobiol. 2011;71: 1102–1130. doi:10.1002/dneu.20935

3. Walma DAC, Yamada KM. The extracellular matrix in development. Development. 2020;147: dev175596. doi:10.1242/dev.175596

4. Waring GL. Morphogenesis of the eggshells in Drosophila. Int Rev Cytol. 2000;198: 67–108. doi:10.1016/s0074-7696(00)98003-3

5. Merkle JA, Wittes J, Schüpbach T. Signaling between somatic follicle cells and the germline patterns the egg and embryo of Drosophila. Curr Top Dev Biol. 2019;140: 55–86. doi:10.1016/bs.ctdb.2019.10.004

6. Narasimha S, Nagornov KO, Menin L, Mucciolo A, Rohwedder A, Humbel BM, et al. Drosophila melanogaster cloak their eggs with pheromones, which prevents cannibalism. PLoS Biol. 2019;17: e2006012. doi:10.1371/journal.pbio.2006012

7. Stein DS, Stevens LM. Maternal control of the Drosophila dorsal–ventral body axis. Wiley Interdiscip Rev: Dev Biol. 2014;3: 301–330. doi:10.1002/wdev.138

8. Fakhouri M, Elalayli M, Sherling D, Hall JD, Miller E, Sun X, et al. Minor proteins and enzymes of the Drosophila eggshell matrix. Dev Biol. 2006;293: 127–141. doi:10.1016/j.ydbio.2006.01.028

9. Pascucci T, Perrino J, Mahowald AP, Waring GL. Eggshell assembly in Drosophila: processing and localization of vitelline membrane and chorion proteins. Dev Biol. 1996;177: 590–598. doi:10.1006/dbio.1996.0188

10. Fargnoli J, Waring GL. Identification of vitelline membrane proteins in Drosophila melanogaster. Dev Biol. 1982;92: 306–314. doi:10.1016/0012-1606(82)90177-4

11. Andrenacci D, Cernilogar FM, Taddei C, Rotoli D, Cavaliere V, Graziani F, et al. Specific domains drive VM32E protein distribution and integration in Drosophila eggshell layers. J Cell Sci. 2001;114: 2819–2829. doi:10.1242/jcs.114.15.2819

12. Alatortsev VE. New genes for vitelline membrane proteins in Drosophila. Mol Biol. 2006;40: 330–332. doi:10.1134/s002689330602021x

13. Jiménez G, González-Reyes A, Casanova J. Cell surface proteins Nasrat and Polehole stabilize the Torso-like extracellular determinant in Drosophila oogenesis. Gene Dev. 2002;16: 913–918. doi:10.1101/gad.223902

621 14. Ventura G, Furriols M, Martín N, Barbosa V, Casanova J. closca, a new gene
622 required for both Torso RTK activation and vitelline membrane integrity. Germline
623 proteins contribute to Drosophila eggshell composition. Dev Biol. 2010;344: 224–
624 232. doi:10.1016/j.ydbio.2010.05.002

625 15. Furriols M, Casanova J. Germline and somatic vitelline proteins colocalize in
626 aggregates in the follicular epithelium of Drosophila ovaries. Fly. 2014;8: 113–119.
627 doi:10.4161/fly.29133

628 16. Tootle TL, Williams D, Hubb A, Frederick R, Spradling A. Drosophila eggshell
629 production: identification of new genes and coordination by Pxt. PLoS One. 2011;6:
630 e19943. doi:10.1371/journal.pone.0019943

631 17. Cavaliere V, Bernardi F, Romani P, Duchi S, Gargiulo G. Building up the
632 Drosophila eggshell: First of all the eggshell genes must be transcribed. Dev Dyn.
633 2008;237: 2061–2072. doi:10.1002/dvdy.21625

634 18. Manogaran A, Waring GL. The N-terminal prodomain of sV23 is essential for the
635 assembly of a functional vitelline membrane network in Drosophila. Dev Biol.
636 2004;270: 261–71. doi:10.1016/j.ydbio.2004.02.009

637 19. Petri WH, Wyman AR, Kafatos FC. Specific protein synthesis in cellular
638 differentiation III. The eggshell proteins of Drosophila melanogaster and their
639 program of synthesis. Dev Biol. 1976;49: 185–199. doi:10.1016/0012-
640 1606(76)90266-9

641 20. LeMosy EK, Hashimoto C. The Nudel protease of Drosophila is required for
642 eggshell biogenesis in addition to embryonic patterning. Dev Biol. 2000;217: 352–
643 361. doi:10.1006/dbio.1999.9562

644 21. Heifetz Y, Yu J, Wolfner MF. Ovulation triggers activation of Drosophila oocytes.
645 Dev Biol. 2001;234: 416–424. doi:10.1006/dbio.2001.0246

646 22. Mindrinos MN, Petri WH, Galanopoulos VK, Lombard MF, Margaritis LH.
647 Crosslinking of the Drosophila chorion involves a peroxidase. Wilhelm Roux Arch
648 Dev Biol. 1980;189: 187–196. doi:10.1007/bf00868677

649 23. Heinecke JW. Tyrosyl radical production by myeloperoxidase: a phagocyte
650 pathway for lipid peroxidation and dityrosine cross-linking of proteins. Toxicology.
651 2002;177: 11–22. doi:10.1016/s0300-483x(02)00192-0

652 24. Hall HG. Hardening of the sea urchin fertilization envelope by peroxidase-
653 catalyzed phenolic coupling of tyrosines. Cell. 1978;15: 343–355. doi:10.1016/0092-
654 8674(78)90003-x

655 25. Han Q, Li G, Li J. Purification and characterization of chorion peroxidase from
656 Aedes aegypti eggs. Arch Biochem Biophys. 2000;378: 107–115.
657 doi:10.1006/abbi.2000.1821

658 26. Bauer BJ, Waring GL. 7C female sterile mutants fail to accumulate early eggshell
659 proteins necessary for later chorion morphogenesis in Drosophila. Dev Biol.
660 1987;121: 349–358. doi:10.1016/0012-1606(87)90171-0

661 27. Hawley RJ, Waring GL. Cloning and analysis of the dec-1 female-sterile locus, a
662 gene required for proper assembly of the Drosophila eggshell. Gene Dev. 1988;2:
663 341–349. doi:10.1101/gad.2.3.341

664 28. Savant SS, Waring GL. Molecular analysis and rescue of a vitelline membrane
665 mutant in Drosophila. Dev Biol. 1989;135: 43–52. doi:10.1016/0012-1606(89)90156-
666 5

667 29. D'Alterio C, Tran DDD, Yeung MWYA, Hwang MSH, Li MA, Arana CJ, et al.
668 Drosophila melanogaster Cad99C, the orthologue of human Usher cadherin
669 PCDH15, regulates the length of microvilli. J Cell Biol. 2005;171: 549–58.
670 doi:10.1083/jcb.200507072

671 30. Schlichting K, Wilsch-Bräuninger M, Demontis F, Dahmann C. Cadherin Cad99C
672 is required for normal microvilli morphology in Drosophila follicle cells. J Cell Sci.
673 2006;119: 1184–95. doi:10.1242/jcs.02831

674 31. Claycomb JM, Benasutti M, Bosco G, Fenger DD, Orr-Weaver TL. Gene
675 amplification as a developmental strategy: isolation of two developmental amplicons
676 in Drosophila. Dev Cell. 2004;6: 145–55.

677 32. Elalayli M, Hall JD, Fakhouri M, Neiswender H, Ellison TT, Han Z, et al. Palisade
678 is required in the Drosophila ovary for assembly and function of the protective
679 vitelline membrane. Dev Biol. 2008;319: 359–369. doi:10.1016/j.ydbio.2008.04.035

680 33. Cernilogar FM, Fabbri F, Andrenacci D, Taddei C, Gargiulo G. Drosophila
681 vitelline membrane cross-linking requires the fs(1)Nasrat, fs(1)polehole and chorion
682 genes activities. Dev Genes Evol. 2001;211: 573–580. doi:10.1007/s00427-001-
683 0192-1

684 34. Blumenthal EM. Cloning of the neurodegeneration gene drop-dead and
685 characterization of additional phenotypes of its mutation. Fly. 2008;2: 180–8.

686 35. Peller CR, Bacon EM, Bucheger JA, Blumenthal EM. Defective gut function in
687 drop-dead mutant Drosophila. J Insect Physiol. 2009;55: 834–9.
688 doi:10.1016/j.jinsphys.2009.05.011

689 36. Conway S, Sansone CL, Benske A, Kentala K, Billen J, Broeck JV, et al.
690 Pleiotropic and novel phenotypes in the Drosophila gut caused by mutation of drop-
691 dead. J Insect Physiol. 2018;105: 76–84. doi:10.1016/j.jinsphys.2018.01.007

692 37. Sansone CL, Blumenthal EM. Neurodegeneration in drop-dead mutant
693 Drosophila melanogaster is associated with the respiratory system but not with
694 hypoxia. PLoS One. 2013;8: e68032. doi:10.1371/journal.pone.0068032

695 38. Buchanan RL, Benzer S. Defective glia in the Drosophila brain degeneration
696 mutant drop-dead. Neuron. 1993;10: 839–850. doi:10.1016/0896-6273(93)90200-b

697 39. Benzer S. From the gene to behavior. JAMA. 1971;218: 1015–1022.
698 doi:10.1001/jama.1971.03190200047010

699 40. Sansone CL, Blumenthal EM. Developmental expression of drop-dead is
700 required for early adult survival and normal body mass in Drosophila melanogaster.
701 Insect Biochem Mol Biol. 2012;42: 690–8. doi:10.1016/j.ibmb.2012.06.002

702 41. Dietzl G, Chen D, Schnorrer F, Su K-C, Barinova Y, Fellner M, et al. A genome-
703 wide transgenic RNAi library for conditional gene inactivation in Drosophila. Nature.
704 2007;448: 151–156. doi:10.1038/nature05954

705 42. Wieschaus E, Nusslein-Volhard C. Looking at embryos. In: Roberts DB, editor.
706 Drosophila: a practical approach. Oxford: IRL Press; 1986. pp. 199–227.

707 43. Chou T, Perrimon N. The autosomal FLP-DFS technique for generating germline
708 mosaics in Drosophila melanogaster. Genetics. 1996;144: 1673–1679.
709 doi:10.1093/genetics/144.4.1673

710 44. Page AW, Orr-Weaver TL. Activation of the meiotic divisions in Drosophila
711 oocytes. Dev Biol. 1997;183: 195–207. doi:10.1006/dbio.1997.8506

712 45. Reese MG, Eeckman FH, Kulp D, Haussler D. Improved Splice Site Detection in
713 Genie. J Comput Biol. 1997;4: 311–323. doi:10.1089/cmb.1997.4.311

714 46. Wu T, Manogaran AL, Beauchamp JM, Waring GL. Drosophila vitelline
715 membrane assembly: A critical role for an evolutionarily conserved cysteine in the
716 “VM domain” of sV23. Dev Biol. 2010;347: 360–368.
717 doi:10.1016/j.ydbio.2010.08.037

718 47. Kim JY, Jang W, Lee HW, Park E, Kim C. Neurodegeneration of Drosophila
719 drop-dead mutants is associated with hypoxia in the brain. Genes Brain Behav.
720 2012;11: 177–184. doi:10.1111/j.1601-183x.2011.00743.x

721 48. Queenan AM, Ghabrial A, Schüpbach T. Ectopic activation of torpedo/Egfr, a
722 Drosophila receptor tyrosine kinase, dorsalizes both the eggshell and the embryo.
723 Development. 1997;124: 3871–3880. doi:10.1242/dev.124.19.3871

724

725

Supporting information

S1 File. Protocol for neutral red permeability assay.

S2 File. Raw numerical data. The six tabs in the spreadsheet contain underlying data for figure S2, table 1, figure 2, figure 5, table 2, and figure 6, respectively.

S1 Fig. Mutation in the *drd*^{1} allele. Upper sequence shows the wild-type sequence of the final five bases of exon 8 (bold), all of intron 8, and the first five bases of exon 9 (bold). The lower sequence shows the same region in *drd*^{1}, with the single base change (green, underlined) and the new start of exon 9 (bold).

S2 Fig. Egg-laying by *drd* mutant females. (A) Fraction of females in each condition that laid any eggs during their lifetime. Because some non yeast-fed females were assayed in groups of 2-3, the data were analyzed with two different assumptions regarding the distribution of egg-laying (see methods). Brackets indicate the effect of yeast feeding (two-sided Fisher's exact test). (B) Number of eggs laid per female, omitting data from those females that laid no eggs. Brackets indicate the effect of yeast feeding (Kruskal-Wallis test with Dunn's post-hoc multiple comparisons test). n=21-67 females per condition.

S3 Fig. Control for *drd* expression in the egg chamber. (A) Maximum intensity projection of a stage 14 egg chamber in which expression of a nuclear GFP reporter is driven by *drd-GAL4*. (B) Control stage 14 egg chamber with the nuclear GFP reporter but no *drd-GAL4* driver.

751 **S1_raw_images. Images of Western blots used in figures 3, 4, and 7.**

752

753 **Figure 1**

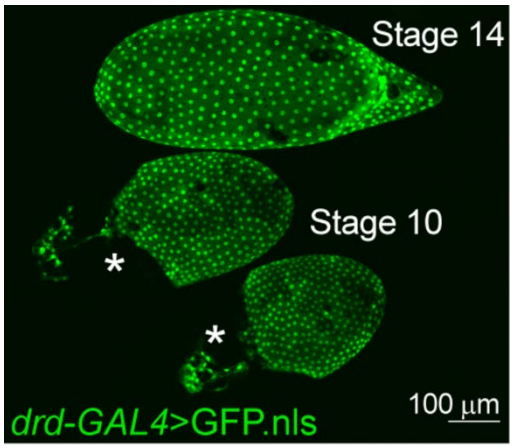

754

755

Figure 2

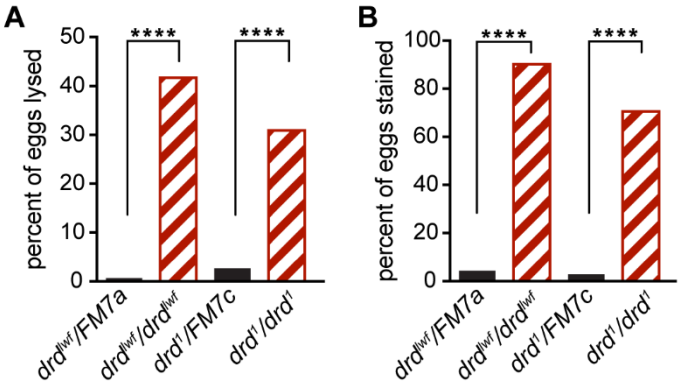

759 **Figure 3**

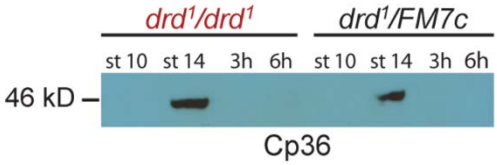

760

761

762 **Figure 4**

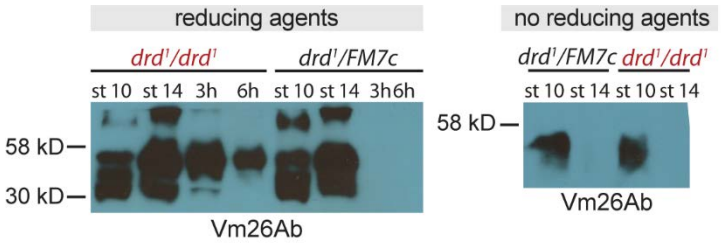

763

764

765 **Figure 5**

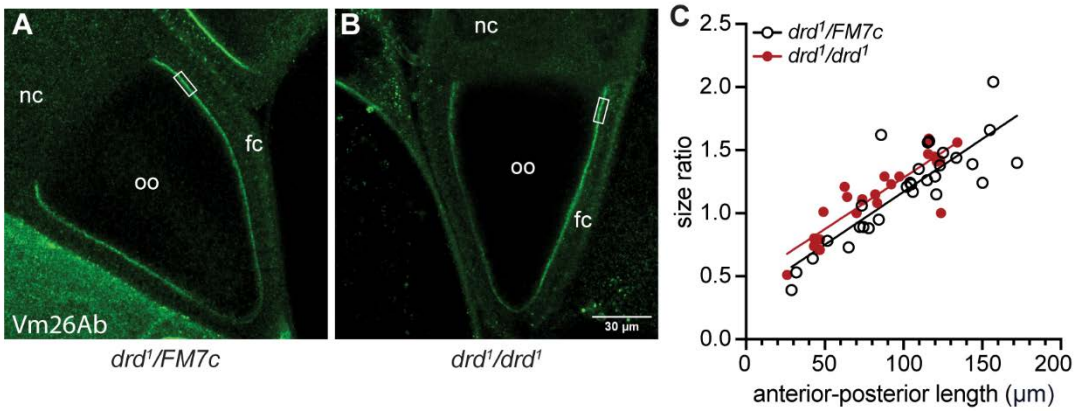

drd¹/FM7c drd¹/drd¹

766

767

768 **Figure 6**

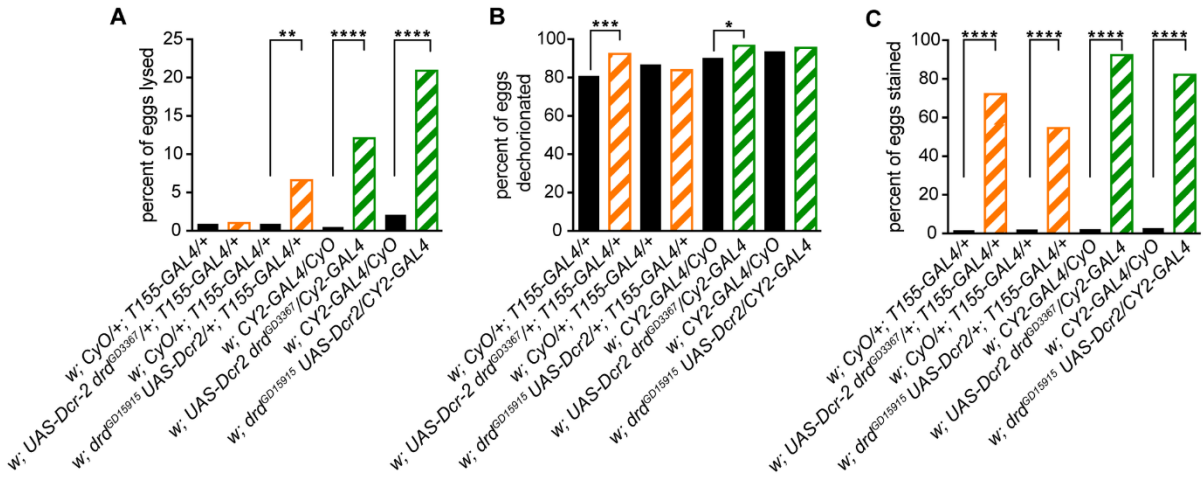

769

770

771 **Figure 7**

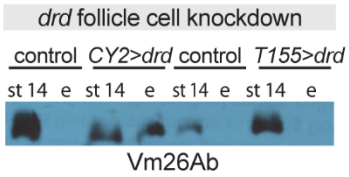

772

773

774 **Figure 8**

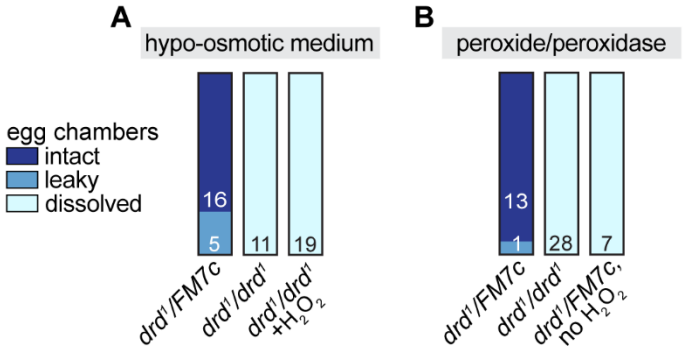

775

776

Figure S1

wild-type

TAATTGTAGGTATTCGCCCAGGTCTAGCATTTATAGAGAATTGTATTTTTTGTTGTTTTTTATTTGCTCAACGCAGCTCGA

***drd*^{1}**

TAATTGTAGGTATTCGCCCAGGTCTAGCATTTATAGAGAATTGTATTTTTTGTTGTTTTTTATTAGCTCAACGCAGCTCGA

783 **Figure S2**
784

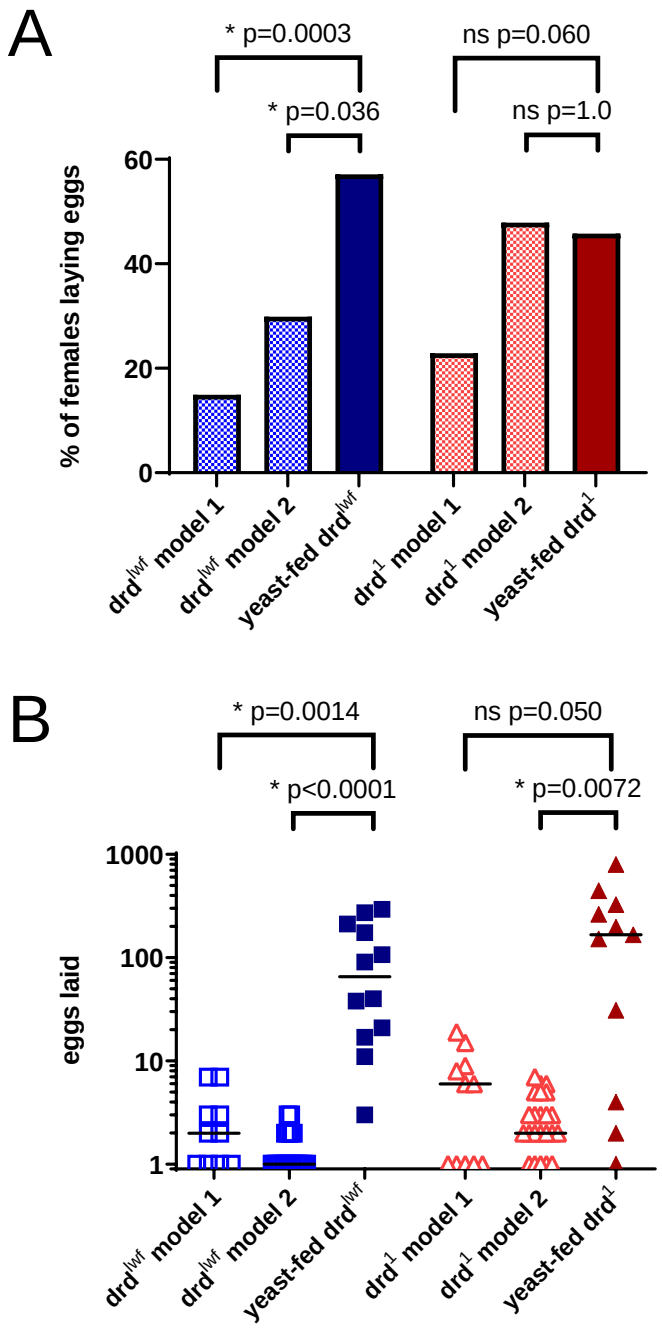

785

786 **Figure S3**

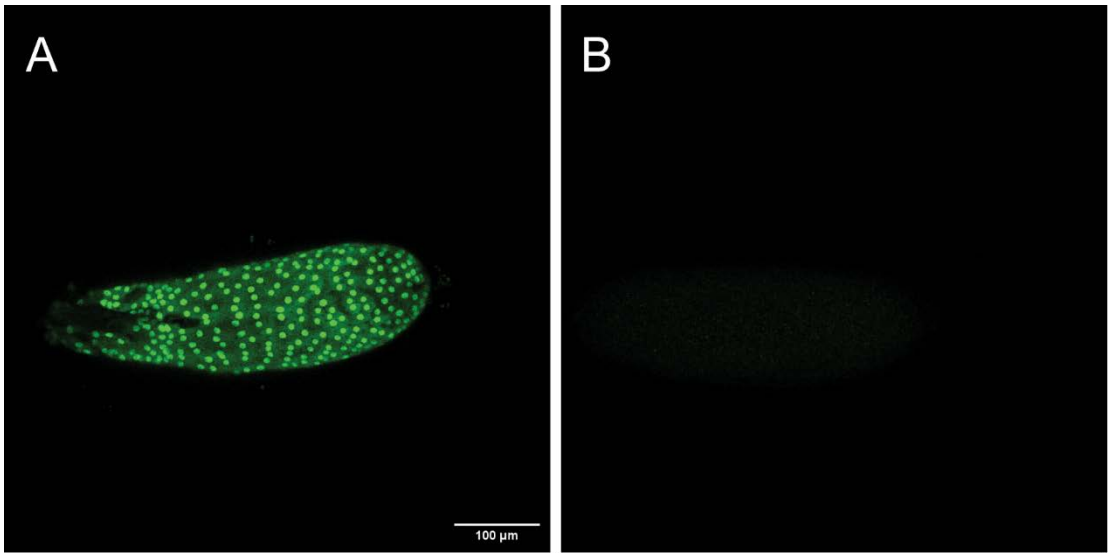

787